Surface acoustic wave generation in *ZX*-cut $LiNbO_3$ superlattices using coplanar electrodes

Didit Yudistira,[1,a)] Sarah Benchabane,[1] Davide Janner,[1] and Valerio Pruneri[1,2]
[1]*ICFO-Institut de Ciencies Fotoniques, Mediterranean Technology Park, Castelldefels, 08860 Barcelona, Spain*
[2]*ICREA-Institució Catalana de Recerca i Estudis Avançats, 08010 Barcelona, Spain*

(Received 27 April 2009; accepted 17 June 2009; published online 3 August 2009)

We report on a configuration to generate surface acoustic waves (SAWs) in acoustic superlattices based on *ZX*-cut periodically poled lithium niobate. The coplanar electrode configuration allows inducing Rayleigh type SAWs with the elastic energy mainly concentrated in between the electrodes gap and under the crystal surface. With respect to standard interdigitated transducers using the same crystal orientation, the efficiency of the SAW generation in the proposed designs are similar, while, for the same grating period, the resonance frequency that can be achieved is two times larger. © *2009 American Institute of Physics*. [DOI: 10.1063/1.3190518]

Periodically poled lithium niobate (PPLN) is an artificially engineered material where domain inversion is usually achieved through *ad hoc* electrical poling techniques.[1] It has been widely used in the field of nonlinear optics, including quasiphase-matched second harmonic generation[1] and optical parametric oscillation.[2] Domain inversion combined with low loss optical waveguides has also been exploited in integrated devices, such as parametric generation of entangled photons[3] and broadband low voltage electro-optic modulation.[4] In acoustics, PPLN has made it possible to induce electromechanical coupling in new configurations,[5] named acoustic superlattices (ASLs), which significantly differ from more common interdigitated transducers (IDTs) (Ref. 6) or bulk wave resonators[7] in a uniform piezoelectric medium.

In an ASL structure, acoustic waves can be launched using uniform electrodes, instead of periodic electrodes, such as in the case of IDTs: domain inversion indeed allows switching the sign, from positive to negative, of all odd rank tensors, particularly of the piezoelectric tensor (e), from one domain to the next, while keeping all even rank tensors, such as permittivity (ε) or elastic constant (c), unaltered. Therefore, the application of a uniform external electric field to the periodic structure will subject the domain walls to a periodic strain resulting from the periodic change in the piezoelectric coefficient, effectively resulting in localized sound sources, and hence on elastic wave generation.[5] The corresponding stress equation reads

$$T_I = c_{IJ}S_J - (-1)^n e_{Ik}E_k, \tag{1}$$

with $I,J=1,2,\ldots,6$ and $n=1,2,3,\ldots,N$, where N is the number of periods, E_k is the k component of the electric field, T_I and S_J are the second rank stress and strain tensor, respectively.

One of the main advantages of ASL based transducers is the fact that the elastic wavelength is directly given by the period Λ of the lattices, resulting in an acoustic frequency given by

$$f = v/\lambda, \tag{2}$$

with $\lambda \equiv \Lambda$, where λ is the acoustic wavelength and v the wave velocity. This is a fundamental difference with conventional IDTs, where the operating frequency is inversely proportional to twice the period. Therefore, for the same grating period, the operating frequency that can be achieved with ASL is twice the frequency that can be obtained from standard IDTs.

A wide variety of configurations of ASL have been investigated, which may be divided into in-line and crossed-line schemes,[5] depending on the direction of the applied electric field with respect to the propagation direction of the generated acoustic wave. Most of the reported configurations rely on metallization of the electrodes on opposite faces of the ASL medium hence resulting in a unidirectional electric field across the entire thickness of the substrate. Therefore, depending on the ratio between the piezoelectric substrate thickness and the lattice period, either bulk[5] or plate (Lamb) waves are generated.[8] Surface acoustic waves (SAWs), of the Rayleigh type in particular, have attracted much less attention in ASLs, despite their potential to compete with high frequency SAW resonators and IDTs. Apart from some related work dedicated to indirect coupling of plate waves to surface waves on substrates consisting of a thin piezoelectric layer deposited on an elastic medium,[9] there is no report of SAW generation in a monolithic piezoelectric ASL substrate.

In this letter we report on direct generation of Rayleigh SAW in an ASL made of PPLN. In particular we show that SAW can be efficiently generated using a coplanar electrode geometry (see Fig. 1) that forces the electric field to be confined in the crystal region between the electrodes and close to the substrate surface, instead of inside the bulk, as it was the case for previous ASL configurations using electrodes on the top and bottom of the plate.[5]

The fabricated structure is outlined in Fig. 1. The ASLs were prepared on a 500 μm thick (t) *ZX*-cut $LiNbO_3$ substrate with a period $\Lambda=15$ μm and with total length $L=N\Lambda$ of about 10 mm. The domain inversion was realized through electric field poling.[1–4] For this configuration, given the SAW velocity on *ZX*-cut $LiNbO_3$, i.e., 3795 m/s, we

a)Electronic mail: didit.yudistira@icfo.es.

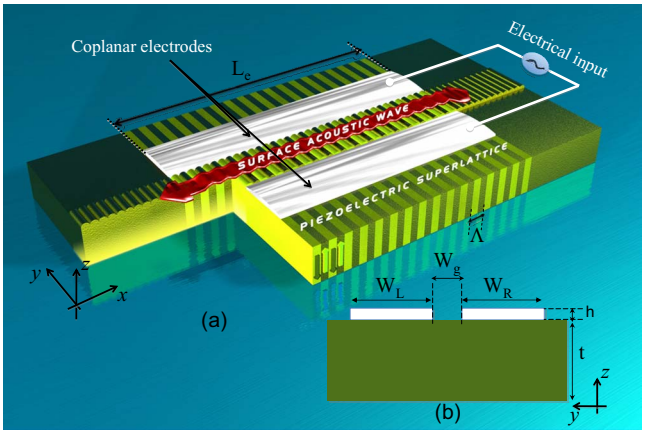

FIG. 1. (Color online) (a) Basic structure of ASL based-on *ZX*-cut PPLN with coplanar aluminum electrodes configuration. (b) Side view (*yz*-plane).

expect a resonance frequency of about 253 MHz. After poling, a pair of coplanar aluminum (Al) electrodes with thickness $h=0.2$ μm was deposited on the ASLs and oriented along the *x*-axis. To minimize acoustic diffraction and by analogy with the rules of thumb usually employed for the acoustic aperture of standard IDTs,[10] the gap width W_g between the electrodes was chosen to be 100 μm, i.e., of a few wavelengths. To avoid parasitic electrical effects, including high resistivity, the electrode width, $W_{L(R)}$, was set to be 100 μm. Various electrodes lengths, L_e, namely 4, 6, 8, and 10 mm, were chosen, while keeping the rest of the parameters fixed, to assess the influence of the ASL length on the transduction efficiency. The electrodes were finally fabricated using a standard lithography process in which an aluminum thin film was sputtered onto the *z*-face of the ASL substrate and photo-lithographically structured through wet etching.

Electrical characterization of the fabricated samples was performed with an Agilent Network Analyzer in the 100–500 MHz frequency range. The reflection scattering parameter S_{11}, and the conductance G_a were measured and compared with those of an unpoled (not domain inverted) *ZX*-cut lithium niobate sample.

A resonance frequency around 253 MHz, as made evident by a strong dip in the electrical response (Fig. 2), was observed, confirming SAW generation as expected. Another

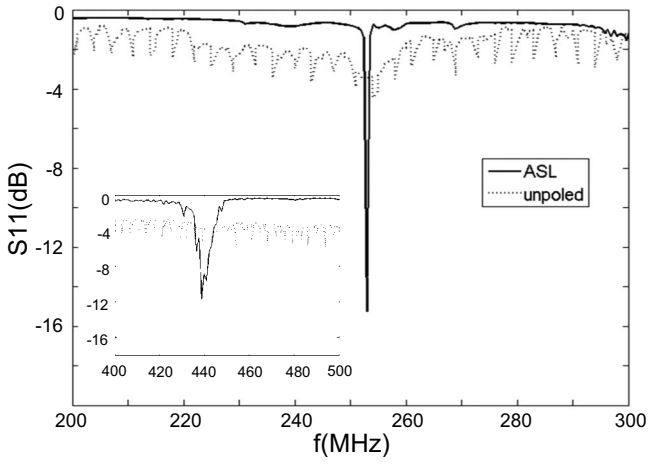

FIG. 2. S_{11} vs f for ASL with length $L_e=10$ mm. Inset shows the corresponding longitudinal bulk wave response.

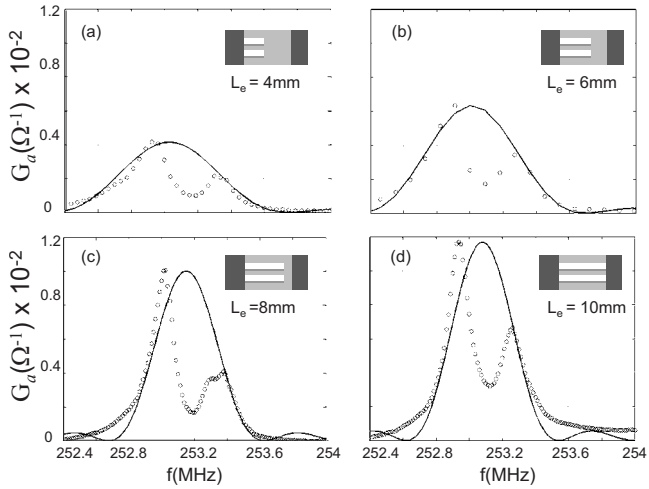

FIG. 3. Conductance (G_a) (circles) of the ASL samples with different electrodes length. Solid lines denote the corresponding fitting curve.

response around 440 MHz was also measured (inset in Fig. 2). From Eq. (2), it can be inferred that the additional high frequency wave has a velocity of about 6600 m/s, which corresponds to the velocity of longitudinal bulk acoustic waves on *ZX*-$LiNbO_3$. This bulk acoustic wave excitation can be accounted for by the fact that the gap width between the electrodes is large enough to allow the applied electric field to penetrate into the substrate, thus transferring energy into the bulk. As expected, acoustic wave generation was not observed from unpoled samples using the same electrode configuration (Fig. 2).

The corresponding conductance G_a for various electrodes length is given in Fig. 3, where each inset shows schematics of the measured device illustrating the electrode length. As expected, a strong peak around the resonance frequency is obtained, indicating optimum transduction in the form of SAW generation. The presence of the side lobe in Fig. 3 might be due to the E_z field component along the electrode. Further experiments are being carried out to explain this effect. The value of G_a at the resonance frequency increases with the electrode length L_e and is maximized for $L_e=10$ mm [Fig. 3(d)], as a consequence of a maximum overlap between the electrodes and the ASL domain. The transduction efficiency can be estimated by determining the effective electromechanical coupling coefficient (K^2_{eff}) of each ASL structure. By fitting the experimentally obtained conductance G_a the K^2_{eff} of the ASLs as a function of electrodes length L_e was calculated and is reported in Fig. 4. The average K^2_{eff} obtained is approximately 0.3% while a value of 0.53% was obtained from the calculation,[11] but, as shown in Fig. 4, K^2_{eff} decreases as the length of the electrodes increases, indicating that the overlap between electrodes and inverted domains is not the only parameter to be taken into account for device optimization. A possible explanation for this dependence on length lies in the increase of diffraction losses with propagation distance as well as in the existence of imperfections in the ASL structure.

To investigate the characteristics of the displacement field for the generated SAW, a full three-dimensional (3D) finite element analysis was performed. The simulations were implemented in COMSOL MULTIPHYSICS, where the geometrical and physical parameters were taken from the actual device. The computational domain was reduced to a unit cell

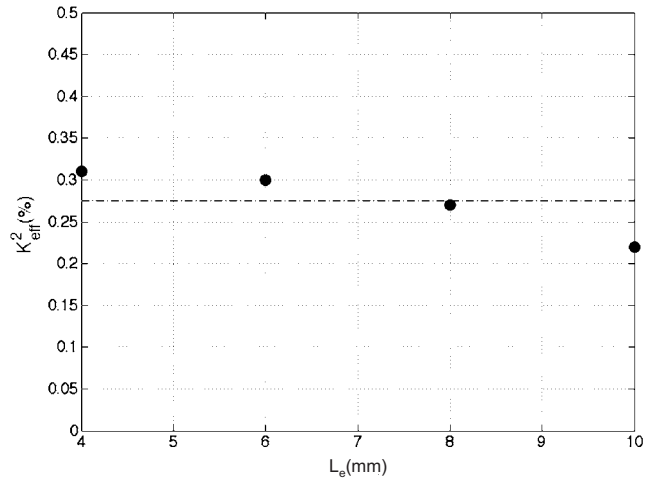

FIG. 4. K^2_{eff} as a function of the electrode length (L_e), with dashed-line denoting the average K^2_{eff}.

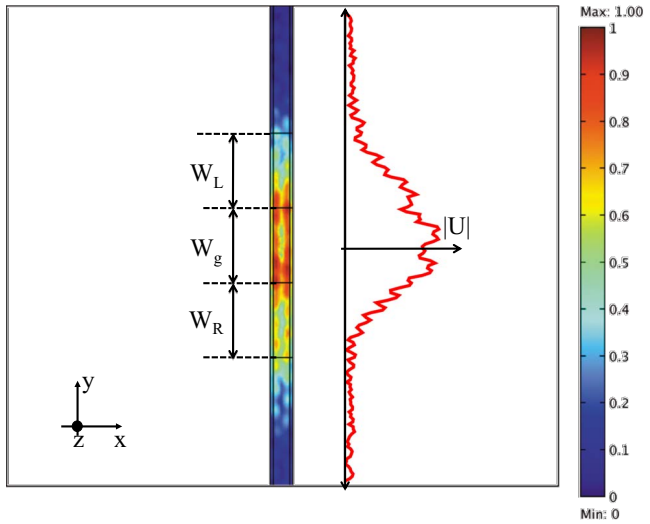

FIG. 5. (Color online) Top view of normalized magnitude of elastic displacements at a frequency of 252.97 MHz.

with periodic boundary conditions in the direction of wave propagation. The simulations predict a SAW at an eigenfrequency of 252.97 MHz, which is in agreement with the SAW resonance frequency reported in our measurements. The corresponding eigenmode that shows the distribution of the displacement field is shown in Fig. 5. It is interesting to note that the displacement (Fig. 5) is mostly confined within the electrode gap and only a very small fraction of the energy propagates outside. In other words, the wave is channeled within the free space in between the electrodes, which is quite similar to the characteristics of SAW generated with IDTs.

In conclusion, we have presented and investigated a coplanar electrode configuration for Rayleigh type SAW generation in *ZX*-cut $LiNbO_3$ ASL. The demonstrated electromechanical coupling coefficient K^2_{eff} is about 0.3%, similar to that obtained in the same cut $LiNbO_3$ crystal using standard IDTs. The 3D finite element simulation agrees well with the experimental results, thus confirming the Rayleigh nature of the generated SAW.

D.Y. and D.J. acknowledge the support of Generalitat de Catalunya and Spanish Ministry through a studentship and the Juan De la Cierva fellowship programmes, respectively. This work was partially supported by Plan Nacional Grant No. TEC 2007-60185, Acciones Integradas Hispano-Francesa Grant No. HF 2008-0033, and by the French Partenariat Hubert Curien (PHC) PICASSO Grant No. 19220SG. The authors thank Vincent Laude for fruitful discussions.

[1]M. Yamada, N. Nada, and K. Watanabe, Appl. Phys. Lett. **62**, 435 (1993).
[2]L. E. Myers, R. C. Eckardt, M. M. Fejer, and R. L. Byer, J. Opt. Soc. Am. B **12**, 2102 (1995).
[3]G. Fujii, N. Namekata, M. Motoya, S. Kurimura, and S. Inoue, Opt. Express **15**, 12769 (2007).
[4]F. Lucchi, D. Janner, M. Belmonte, S. Balsamo, M. Villa, S. Giurgiola, P. Vergani, and V. Pruneri, Opt. Express **15**, 10739 (2007).
[5]Y. Q. Lu, Y. Zhu, Y. Chen, S. Zhu, N. Ming, and Y. Feng, Science **284**, 1822 (1999).
[6]R. M. White and F. W. Voltmer, Appl. Phys. Lett. **7**, 314 (1965).
[7]Z. Yan, X. Y. Zhou, G. K. H. Pang, T. Zhang, W. L. Liu, J. G. Cheng, Z. T. Song, S. L. Feng, L. H. Lai, and Y. Wang, Appl. Phys. Lett. **90**, 143503 (2007).
[8]E. Courjon, N. Courjal, W. Daniau, G. Lengaigne, L. Gauthier-Manuel, S. Ballandras, and J. Hauden, J. Appl. Phys. **102**, 114107 (2007).
[9]A. K. S. Kumar, P. Paruch, J. M. Triscone, W. Daniau, S. Ballandras, L. Pellegrino, D. Marre, and T. Tybell, Appl. Phys. Lett. **85**, 1757 (2004).
[10]T. L. Szabo and A. J. Slobodnik, Jr., IEEE Trans. Sonics Ultrason. **20**, 240 (1973).
[11]A. J. Slobodnik, E. D. Conway, and R. T. Delmonico, *Microwaves Acoustic Handbook* (Air Force Cambridge Research Laboratories Hanscom, Bedford, MA, 1973), TR-73-0597.